doi:10.1038/nature10754

Supplementary note 1

To compare our data with previous studies, we measured the width of spikes from identified dopaminergic neurons and unidentified neurons from *DAT*-Cre mice. Previous studies used a criterion that dopaminergic neurons should have wide spikes. We found significant diversity in spike waveforms from identified dopaminergic neurons (Fig. S4). There was no significant difference across neuron types in spike duration (ANOVA $F_{2,89} = 0.15$, $P > 0.7$). We found that *Type I* neurons (and identified dopaminergic neurons, when considered separately) had lower baseline firing rates than *Types II* or *III* neurons (*Type II* - *Type I* mean ± 95% CI, 6.73 ± 6.72 spikes/s, Tukey HSD test, $P < 0.05$; *Type III* - *Type I*, 11.11 ± 8.84 spikes/s, $P < 0.01$), although many *Types II* and *III* neurons had low firing rates (<10 spikes/s). Thus, many identified dopaminergic neurons in the present study would have been missed using previous criteria.

Supplementary note 2

Models of RPE typically assume two excitatory inputs, those from reward-predicting cues (CS) and those from reward (US), in addition to inhibitory inputs reflecting reward expectation discussed above (Fig. S12a). Where do these excitatory inputs come from? That some dopaminergic neurons respond preferentially to reward (and weakly to CS) raises the possibility that these US-preferring neurons may provide other CS-preferring dopaminergic neurons with the reward signals. If this is the case, these neurons should meet the following predictions. First, excitation of these neurons should cause phasic excitation of other dopaminergic neurons (the ones calculating RPE). Second, these neurons should not receive inhibitory inputs encoding reward expectation. First, we observed that the excitation of dopaminergic neurons (using ChR2 stimulation in *DAT*-Cre mice) did not cause synaptic excitation of dopaminergic neurons (Fig. S6d). This result does not support the view that a class of "reward-coding" dopaminergic neurons excites other "RPE-coding" dopaminergic neurons. Second, the magnitude of inhibition during reward omission was as large in US-preferring dopaminergic

neurons as in CS-preferring dopaminergic neurons (Figs. 4, S8, S9). This does not support the view that there is a class of dopaminergic neurons that "purely" encodes reward signals. These results suggest that reward-encoding neurons, as proposed in the models, are located outside the VTA. Similarly, although CS-preferring dopaminergic neurons can, in principle, provide excitatory inputs to other dopaminergic neurons, our results do not support this view, suggesting that excitatory inputs for CS also come from outside the VTA.

Supplementary note 3

Our experiments allow us to map a neuron's function onto the transmitter it releases. The percentage of *Type I* neurons (49/95, or 52%) is close to the estimate of the percentage of dopaminergic neurons in rat VTA (55-65%)[6-8]. Furthermore, the unidentified *Type I* neurons showed similar task-related activity to identified dopaminergic neurons (Fig. S11a,b). Together with the observation that *Type I* neurons, but not *Types II* and *III* neurons, responded to light stimulation in *DAT*-Cre mice, this suggests that unidentified *Type I* neurons were also dopaminergic (although we cannot rule out the possibility that some *Type I* neurons were non-dopaminergic). The second experiment showed that identified GABAergic neurons were of *Type II*. The identity of *Type III* neurons remains to be determined. They may release a different neurotransmitter, such as glutamate[14], but we cannot rule out the possibility that *Type III* neurons are GABAergic or dopaminergic (although the latter seems unlikely, given the high efficiency of ChR2 expression in dopaminergic neurons throughout VTA, regardless of projection target; see Figs. S2, S3).

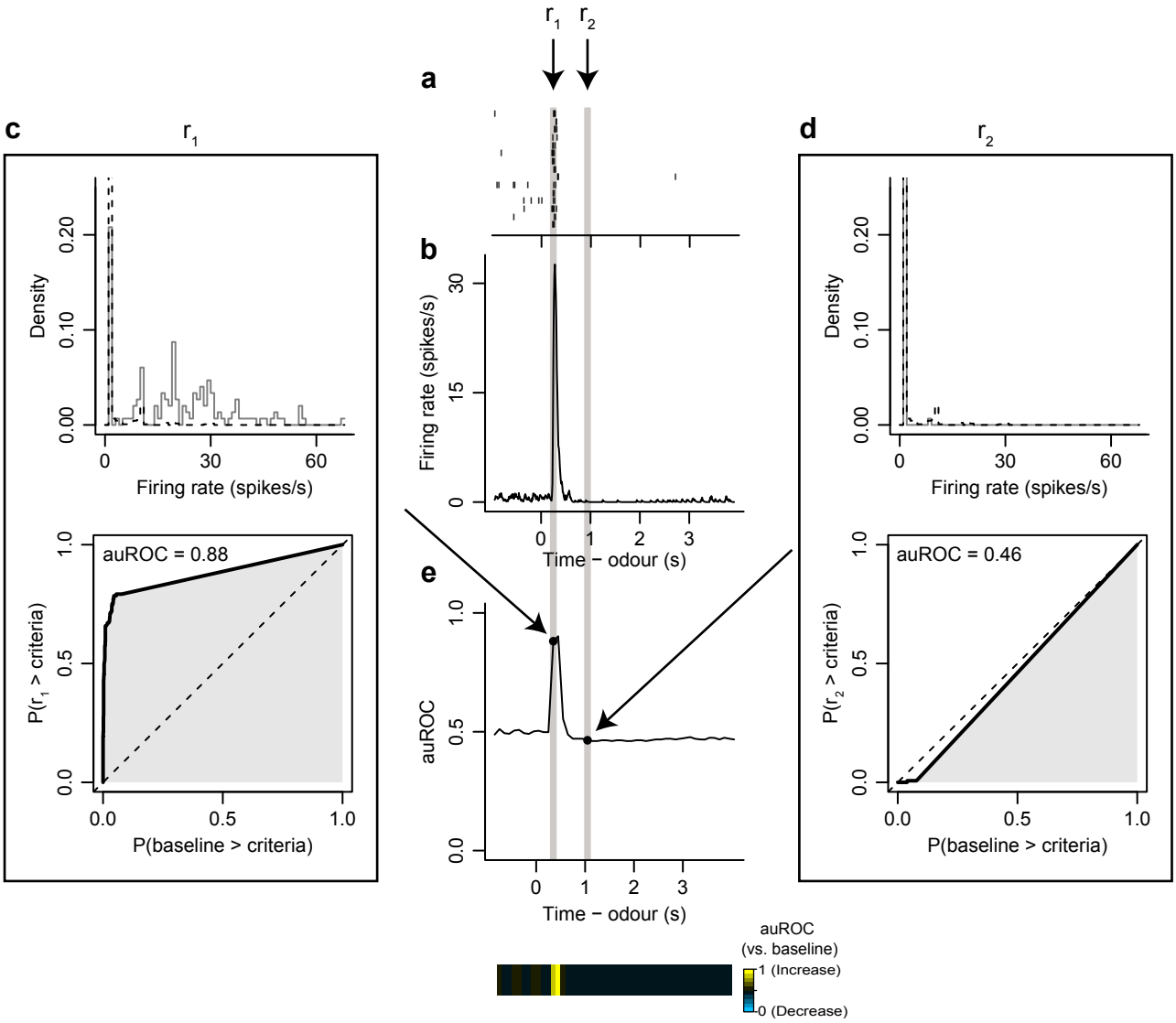

Figure S1. ROC analysis. a, Raster plot from 15 trials of 149 big-reward trials from a dopaminergic neuron. r_1 and r_2 correspond to two example 100-ms bins. **b**, Average firing rate of this neuron. **c**, Area under the receiver operating characteristic curve (auROC) for r_1, in which the neuron increased its firing rate relative to baseline. We compared the histogram of spike counts during the baseline period (dashed line) to that during a given bin (solid line) by moving a criterion from zero to the maximum firing rate (in this example, 68 spikes/s). We then plotted the probability that the activity during r_1 was greater than the criteria against the probability that the baseline activity was greater than the criteria. The area under this curve quantifies the degree of overlap between the two spike count distributions (i.e., the discriminability of the two). The histogram in the top panel is truncated at an ordinate value of 0.2 for display purposes. **d**, Similar to (**c**), but for r_2, which corresponds to an auROC value close to 0.5 (i.e., activity close to baseline). **e**, auROC response profile for the full duration of the task, with r_1 and r_2 indicated by arrows. Shown below are the heat map values, as depicted in Fig. 2.

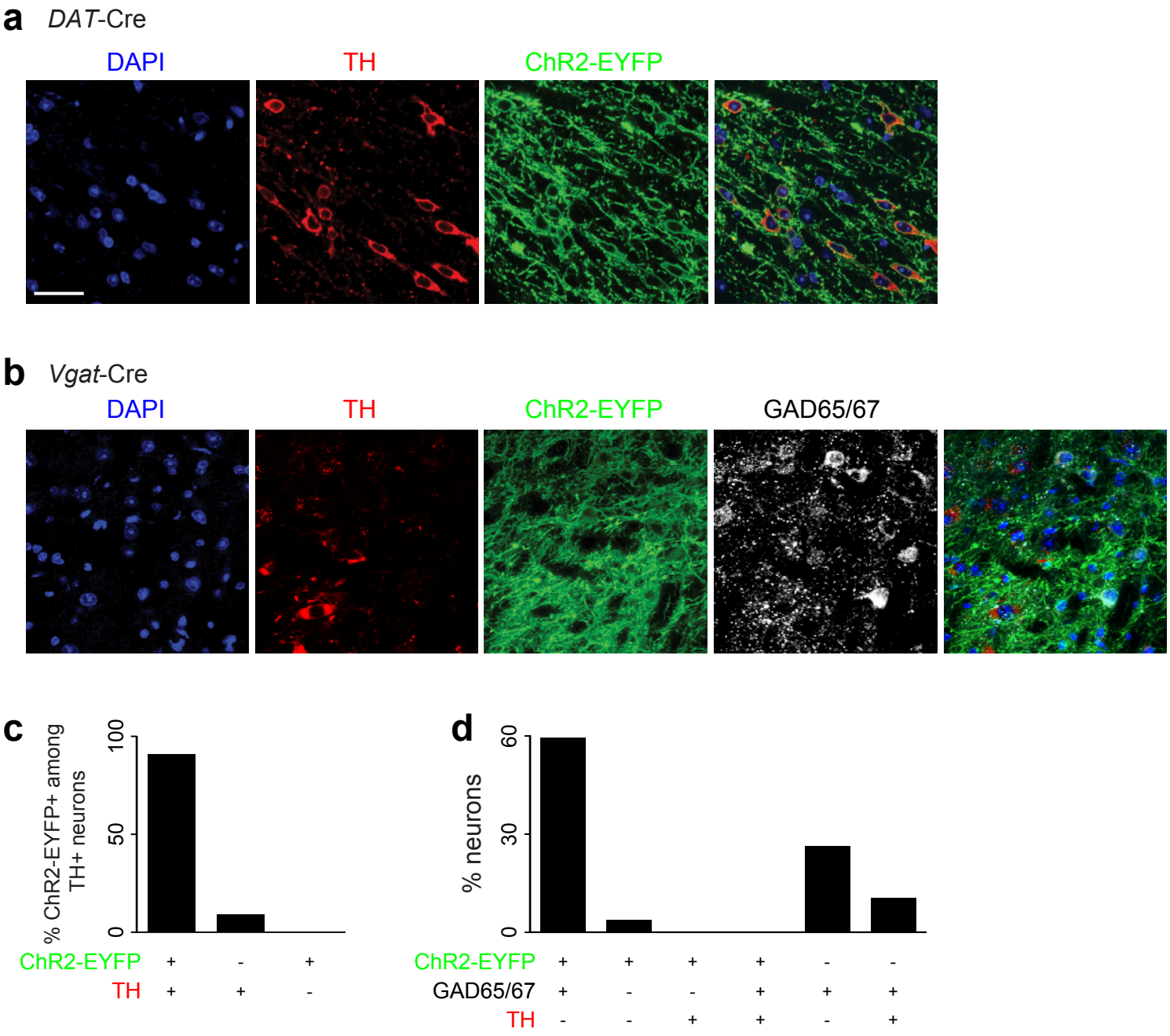

Figure S2. Efficient and specific expression of ChR2-EYFP in dopaminergic and GABAergic neurons. **a**, Blue: DAPI (nuclear marker). Red: immunostaining for TH (dopaminergic neurons). Green: ChR2-EYFP. Scale bar is 50 μm. **b**, Colors as in **a**; White: immunostaining for GAD65/67. Slices are from *DAT*-Cre (**a**) or *Vgat*-Cre (**b**) mice injected with rAAV5-ChR2-EYFP. **c**, Percentage of neurons labeled for EYFP-ChR2 and TH (n = 666 neurons in 2 mice). **d**, Percentage of neurons labeled for EYFP-ChR2, TH and GAD65/67 (n = 433 neurons in 2 mice).

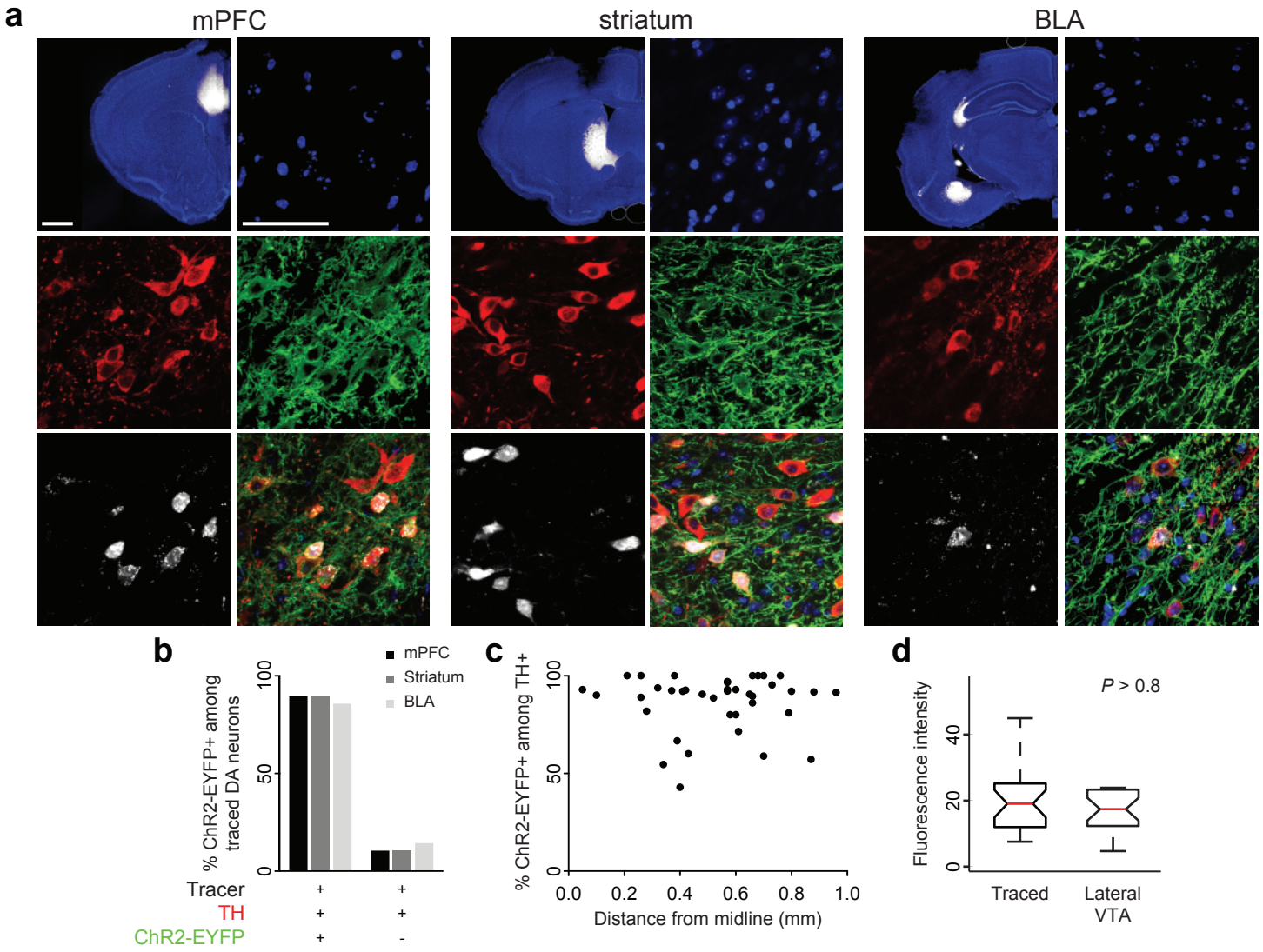

Figure S3. ChR2 expression is uniform across dopaminergic neurons with different projection targets. A recent study found lower levels of DAT in dopaminergic neurons projecting to prefrontal cortex, nucleus accumbens core, and basolateral amygdala versus those projecting to lateral nucleus accumbens shell and dorsolateral striatum[16]. Because Cre expression in the *DAT*-Cre mouse is under the control of the *DAT* gene promoter, this could have biased ChR2 expression toward cells with high *DAT* promoter activity. To confirm that our recordings were not biased toward dopaminergic neurons with a particular projection target, we injected fluorogold, a retrograde tracer, into the prefrontal cortex, striatum, or basolateral amygdala in AAV-FLEX-ChR2-injected *DAT*-Cre mice, and counted the proportion of TH-expressing neurons that also expressed fluorogold and ChR2. **a**, Fluorogold tracing from medial prefrontal cortex (mPFC, left), striatum (middle), and basolateral amygdala (BLA, right) with stains for cell nuclei (To-Pro-3, blue), TH (red), ChR2-EYFP (green), fluorogold (white), and their overlay. Scale bars: 1 mm (left) and 50 μm (right). **b**, The infection efficiency of dopaminergic neurons with identified projection to mPFC, striatum and BLA was similar to the overall infection efficiency measured throughout VTA (Fig. S2). The percentage of VTA neurons triple-labeled by tracer, TH, and ChR2-EYFP was similar across projection target sites, suggesting that virus-mediated ChR2 expression did not preferentially target a subpopulation of dopaminergic neurons (mPFC, n = 67, striatum, n = 145, BLA, n = 35). **c**, Dopaminergic neurons with high *DAT* expression are mainly found in the lateral extent of VTA[21], while low *DAT* expressing neurons are distributed throughout the medial to lateral extent of VTA. Consistent with the finding in (**b**), the viral infection efficiency was similar along the medial-lateral axis of VTA (n = 39). **d**, To evaluate possible differences in cellular ChR2 expression levels, we measured the relative ChR2-EYFP fluorescence intensity over background in dopaminergic neurons projecting to mPFC, BLA or striatum and dopaminergic neurons in the lateral VTA (parabrachial pigmented nucleus). ChR2-EYFP expression was similar in all analysed dopaminergic neurons (n = 25 for each condition).

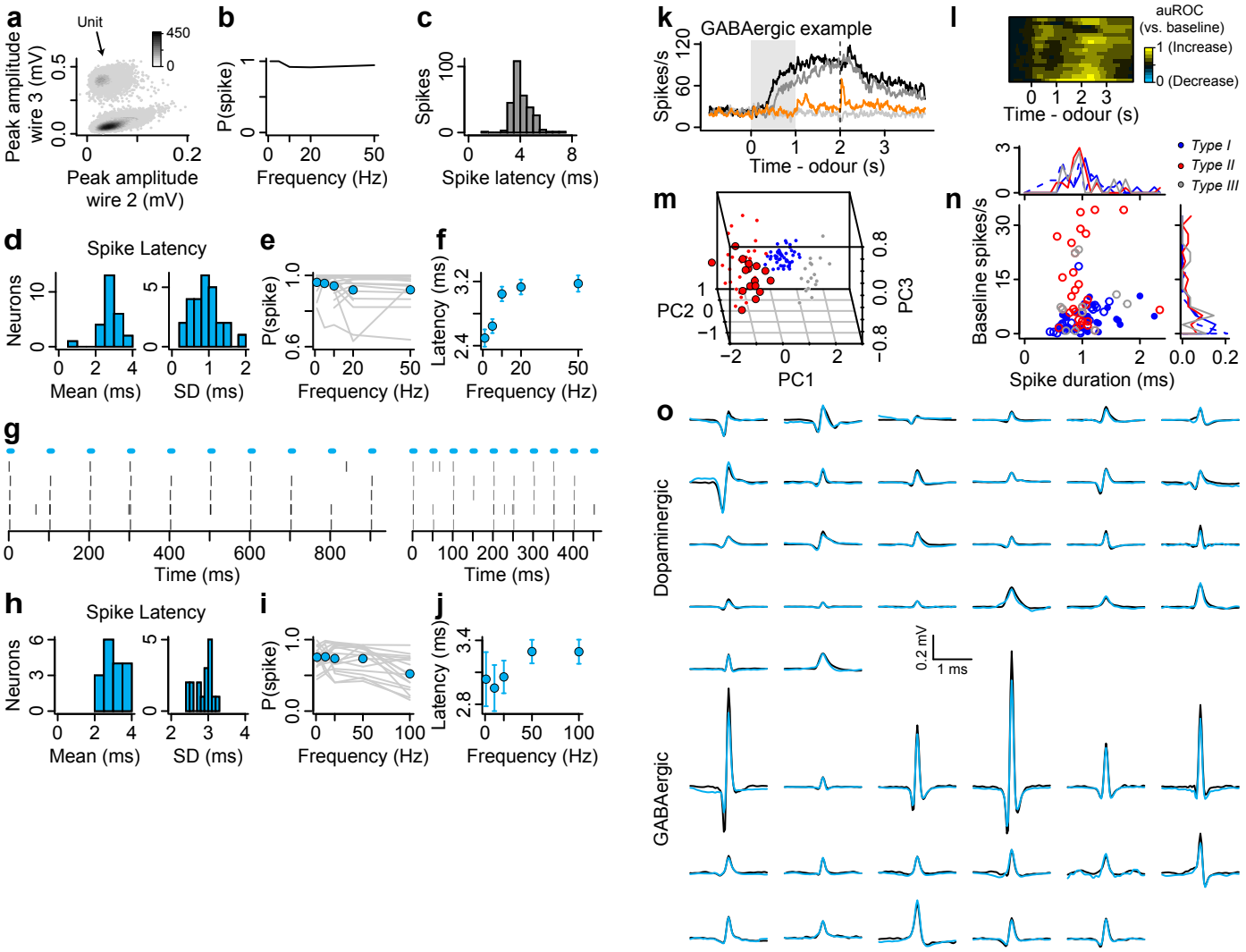

Figure S4. Identification of light-responsive neurons. **a**, Isolation of the neuron in Fig. 3a. Binned scatterplot shows peak amplitude of spike waveforms from two wires of the tetrode. Isolated unit is the upper cluster. The lower cluster is noise. **b**, Probability of a spike (for the second through tenth pulses in each train) as a function of stimulation frequency for this neuron. **c**, Spike latency relative to light onset for this neuron. **d**, Histogram of mean (left) and SD (right) spike latency to light stimulation for 26 identified dopaminergic neurons. **e**, Probability of a spike as a function of stimulation frequency for each dopaminergic neuron (grey) and the mean across dopaminergic neurons (cyan). **f**, Mean ± SEM spike latency as a function of stimulation frequency. **g**, Response from a GABAergic neuron to 5 repetitions of 10 Hz (left) or 20 Hz (right) light stimulation (cyan bars). Ticks represent spikes. **h**, Histogram of mean (left) and SD (right) spike latency to light stimulation for 17 identified GABAergic neurons. **i**, Probability of a spike as a function of stimulation frequency for each GABAergic neuron (grey) and the mean across GABAergic neurons (cyan). **j**, Mean ± SEM spike latency as a function of stimulation frequency. **k**, Response pattern of an example identified GABAergic neuron. **l**, Temporal response profiles of identified GABAergic neurons. Conventions are as in Fig. 2b. **m**, The first three principal components of the auROC curves of all neurons from Fig. 2c (small points) and from identified GABAergic neurons (large points), using the model fit from Fig. 2c. Each GABAergic neuron fell within 95% confidence intervals of the *Type II* cluster defined in *DAT*-Cre mice. **n,** Baseline firing rate vs. spike duration for neurons of each type with density histograms in the margins. Spike duration was calculated as the time at which the voltage was significantly different from baseline (1 ms of pre-spike voltage). **o**, Mean spontaneous (black) and light-evoked (cyan) spike waveforms from 26 identified dopaminergic neurons and 17 identified GABAergic neurons.

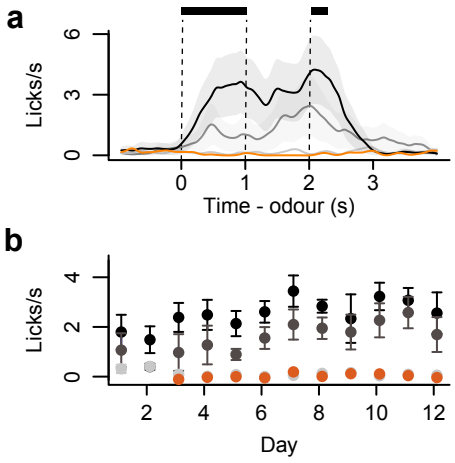

Figure S5. **a**, Licking behaviour from a representative experimental session from a *Vgat*-Cre mouse. Black bars indicate CS and US delivery. Shaded regions around lick traces denote SEM. **b**, mean ± SEM licks during the delay between CS and US as a function of days of the experiment across *Vgat*-Cre animals.

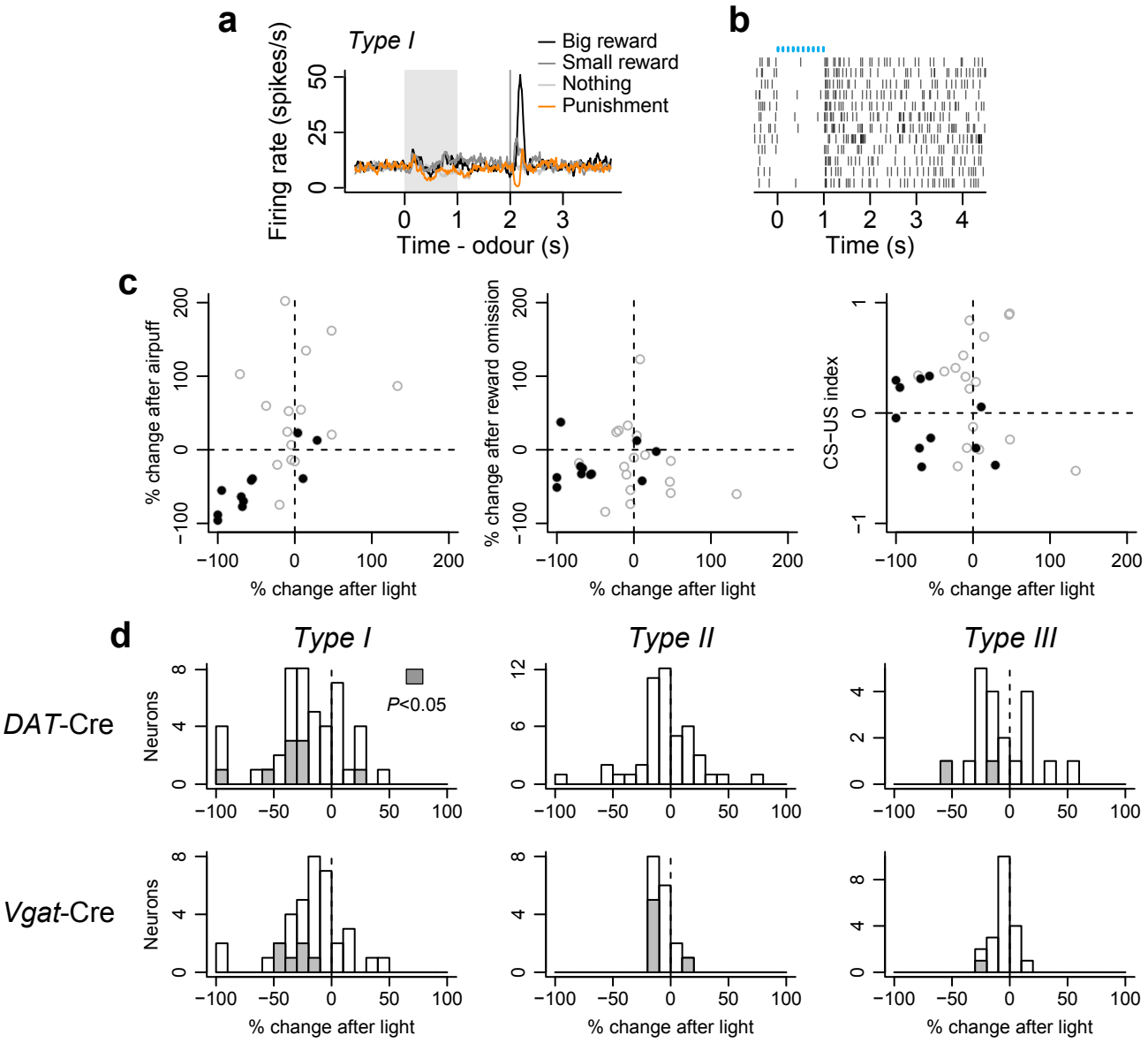

Figure S6. Putative synaptic effects of ChR2 stimulation. **a**, Firing rates from a *Type I* neuron in a *Vgat*-Cre mouse. **b**, Response of the neuron to 12 trials of 10 Hz light pulses (cyan bars). The neuron was inhibited by GABAergic stimulation. **c**, Scatter plots of % change (maximal magnitude of change in the 5-20 ms following light pulses) in firing rate after airpuff, reward omission, and CS-US index vs. % change (maximal magnitude of change) in firing rate after light stimulation in 28 *Type I* neurons from *Vgat*-Cre mice. The 11 neurons for which light stimulation had a significant effect are shown in black (Wilcoxon rank sum test, $P < 0.05$). There was a significant correlation between % change in firing rate after airpuff and % change in firing rate after light stimulation across the population ($r = 0.59$, $P < 0.001$) and for the 11 neurons with a significant response to light stimulation ($r = 0.86$, $P < 0.001$). **d**, % firing rate changes from baseline in the 5-20 ms following all light pulses in *DAT*-Cre (top row) and *Vgat*-Cre (bottom row) mice for each neuron type.

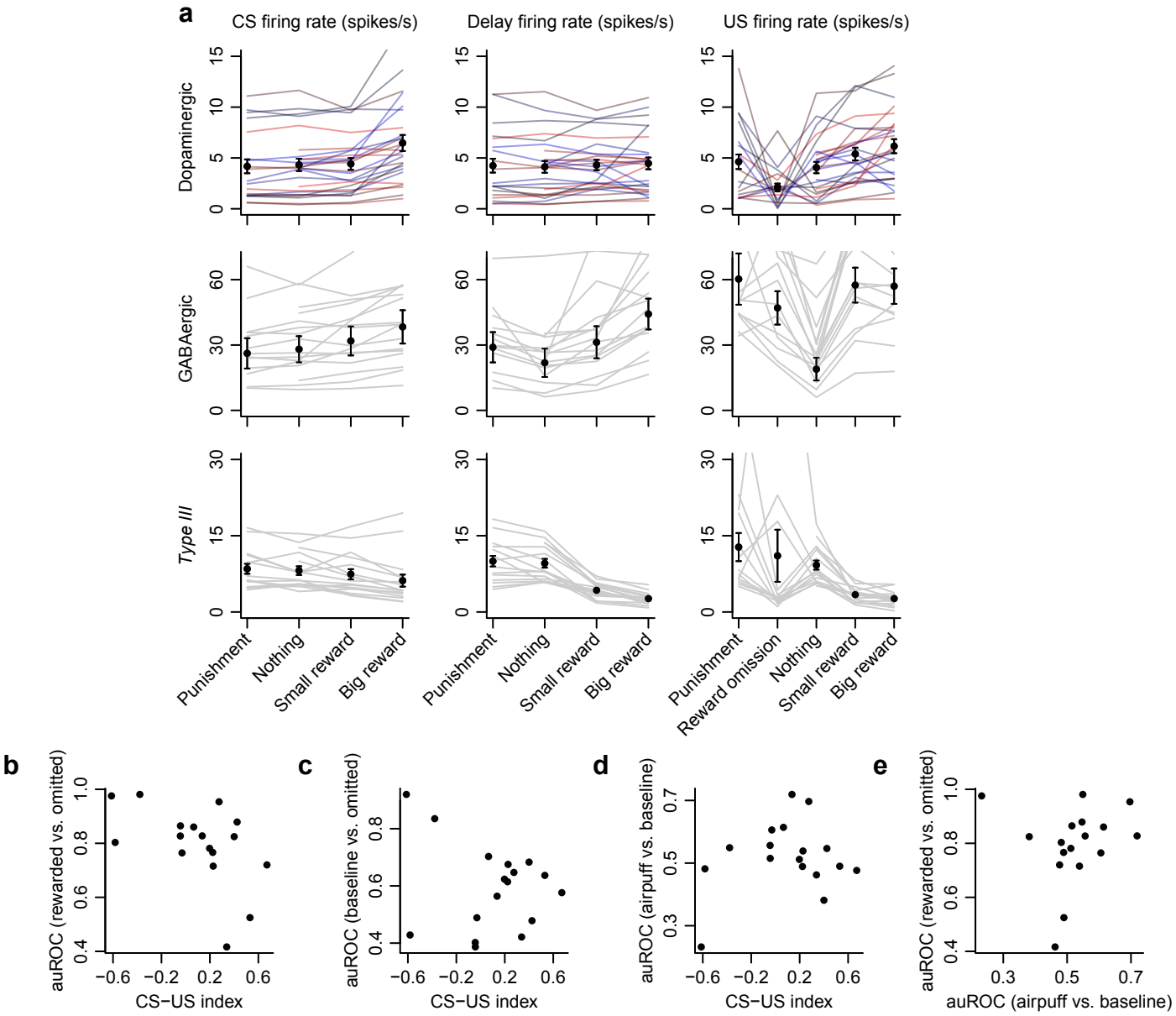

Figure S7. **a**, Mean firing rates for identified dopaminergic (top row), GABAergic (middle row), and *Type III* (bottom row) neurons during CS (left column), delay between CS and US (middle column), and 500 ms after US onset (right column). Each neuron is plotted in grey with the mean and SEM overlaid. Individual dopaminergic neurons are plotted as a function of their CS-US index, with red indicating large CS-US index (i.e., higher firing rate for CS vs. US), blue indicating small CS-US index. **b**, auROC values for reward present compared to reward absent versus CS-US index. There was a significant negative correlation (r = -0.51, P < 0.05) that disappeared with a leverage analysis, indicating that the correlation was driven mostly by one or two neurons. **c**, auROC values for baseline compared to reward absent versus CS-US index. There was no significant correlation. **d**, auROC values for reward present compared to reward absent versus auROC values for airpuff compared to baseline. There was no significant correlation. **e**, auROC values for airpuff compared to baseline versus CS-US index. There was no significant correlation.

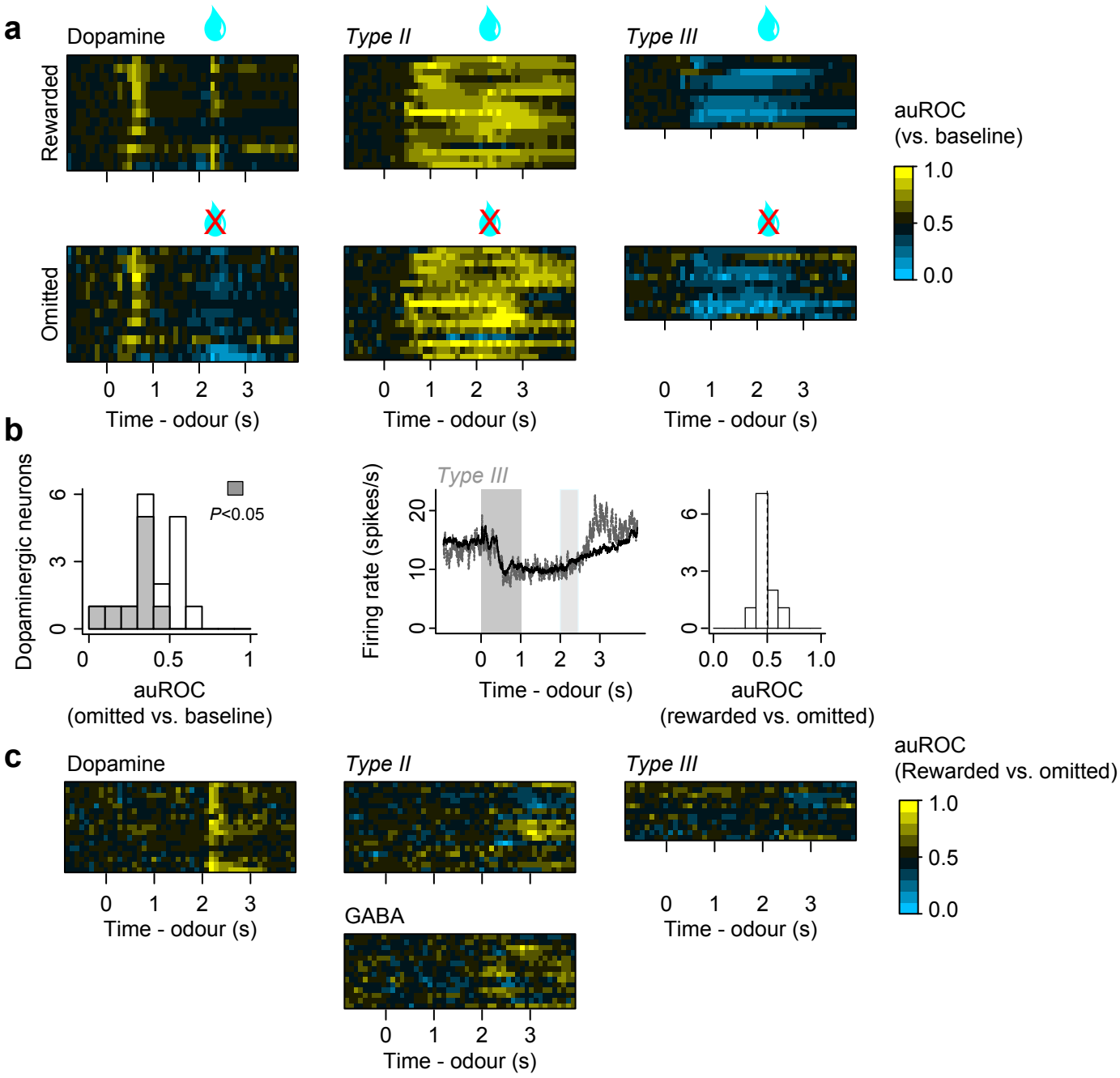

Figure S8. Response profiles of all neurons during reward-omitted trials. **a,** Firing patterns during big-reward trials in which reward was delivered (top) and omitted (bottom). Firing rate changes from baseline were quantified using the auROC curve. Values were computed between each neuron's activity across time and its baseline activity. Yellow: increase from baseline, cyan: decrease from baseline. **b,** Histogram of auROC values during the reward omission period relative to baseline for dopaminergic neurons (left) and example *Type III neuron* and histogram of auROC values for rewarded versus omitted trials. **c,** Difference between rewarded and reward-omitted trials for big-reward trials for identified dopaminergic neurons, unidentified *DAT*-Cre *Types II* and *III* neurons, and identified GABAergic neurons. auROC values were computed between reward-present and reward-absent trials. Each row represents one neuron. Yellow: rewarded > omitted, cyan: rewarded < omitted.

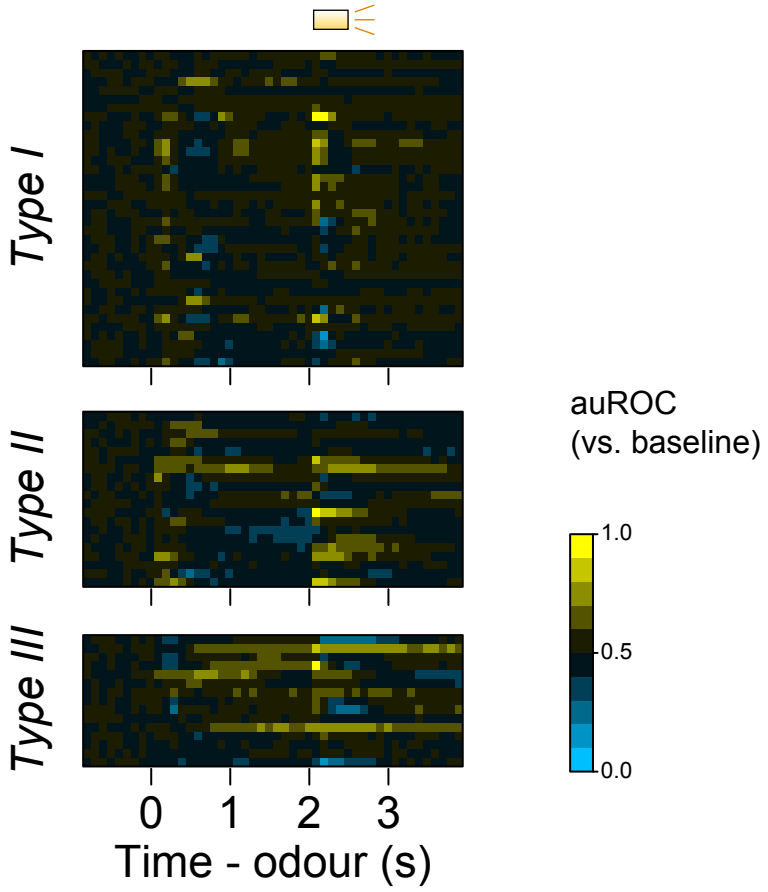

Figure S9. Response profiles of all neurons during airpuff trials. auROC curves for punishment trials relative to baseline activity.

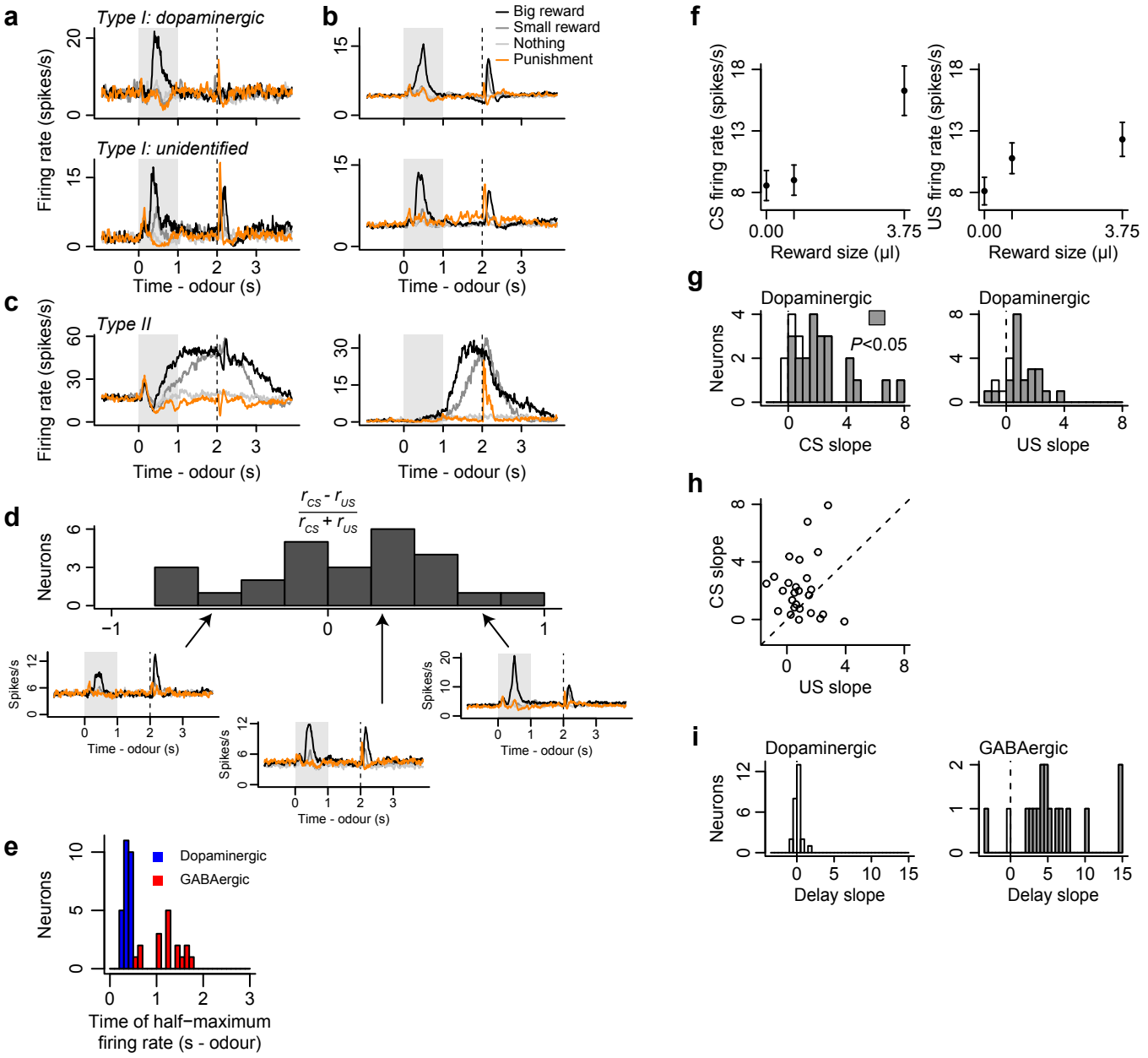

Figure S10. Firing patterns of more example neurons and CS and US responses in dopaminergic neurons. **a**, Examples of firing rates from identified and unidentified *Type I* neurons. **b**, Average firing rates from 26 identified dopaminergic neurons and 23 unidentified *Type I* neurons. **c**, Examples of firing rates from *Type II* neurons. **d**, Average firing rates from the lowest, middle, and upper third of the CS-US index histogram in Fig. 4c (reproduced here). **e**, The time of half-maximum firing rate during big-reward trials from odour onset to reward onset. Identified GABAergic neuron firing rates slowly rose to a peak, while identified dopaminergic neuron firing rates peaked during the CS. **f**, Firing rates for dopaminergic neurons during CS and US. **g**, Regression slopes of the firing rates versus reward size during CS and US for dopaminergic neurons during CS and. **h**, Slope values for each dopaminergic neuron during CS and US. **i**, Slope values during the delay between CS and US. While the delay activity of GABAergic neurons was parametrically modulated by the value of reward, none of identified dopaminergic neurons showed such modulation. Unidentified *Type II* neurons showed a similar modulation by reward value as GABAergic neurons (43/47 unidentified *Type II* neurons showed significant delay-period slope values and 40/47 showed significant differences between no-, small- and big-reward trials, $P < 0.001$).

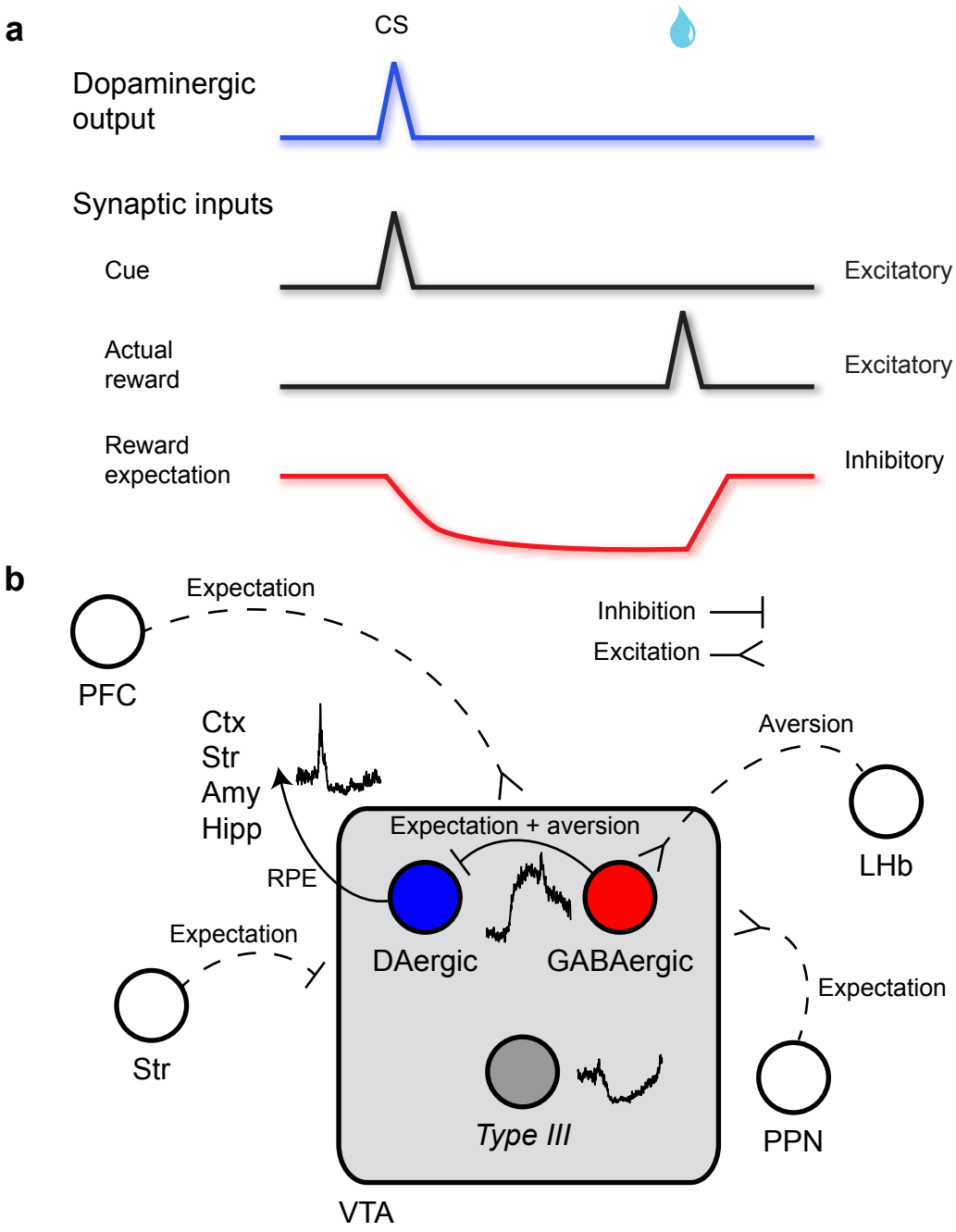

Figure S11. Proposed RPE model and circuit diagram. **a**, A synaptic model of RPE calculation (after Houk et al., 1995). Dopaminergic spikes are a result of excitatory inputs about reward-predicting cues and actual reward, and inhibitory inputs about reward expectation. **b**, Schematic interaction of VTA dopaminergic (DAergic) and GABAergic neurons. VTA receives reward-expectation input from prefrontal cortex (PFC, including orbitofrontal cortex), striatum (str) and pedunculopontine nucleus (PPN). VTA receives inputs about aversive stimuli from lateral habenula (LHb). VTA GABAergic neurons integrate information about reward expectation and aversive stimuli and dopaminergic neurons project RPE signals to cortex (ctx), striatum, amygdala (amy), hippocampus (hipp), and elsewhere. Example firing rates from each type of neuron we recorded are shown. We have omitted many other areas known to be important in this circuit (e.g., rostromedial tegmental nucleus). See text for details.

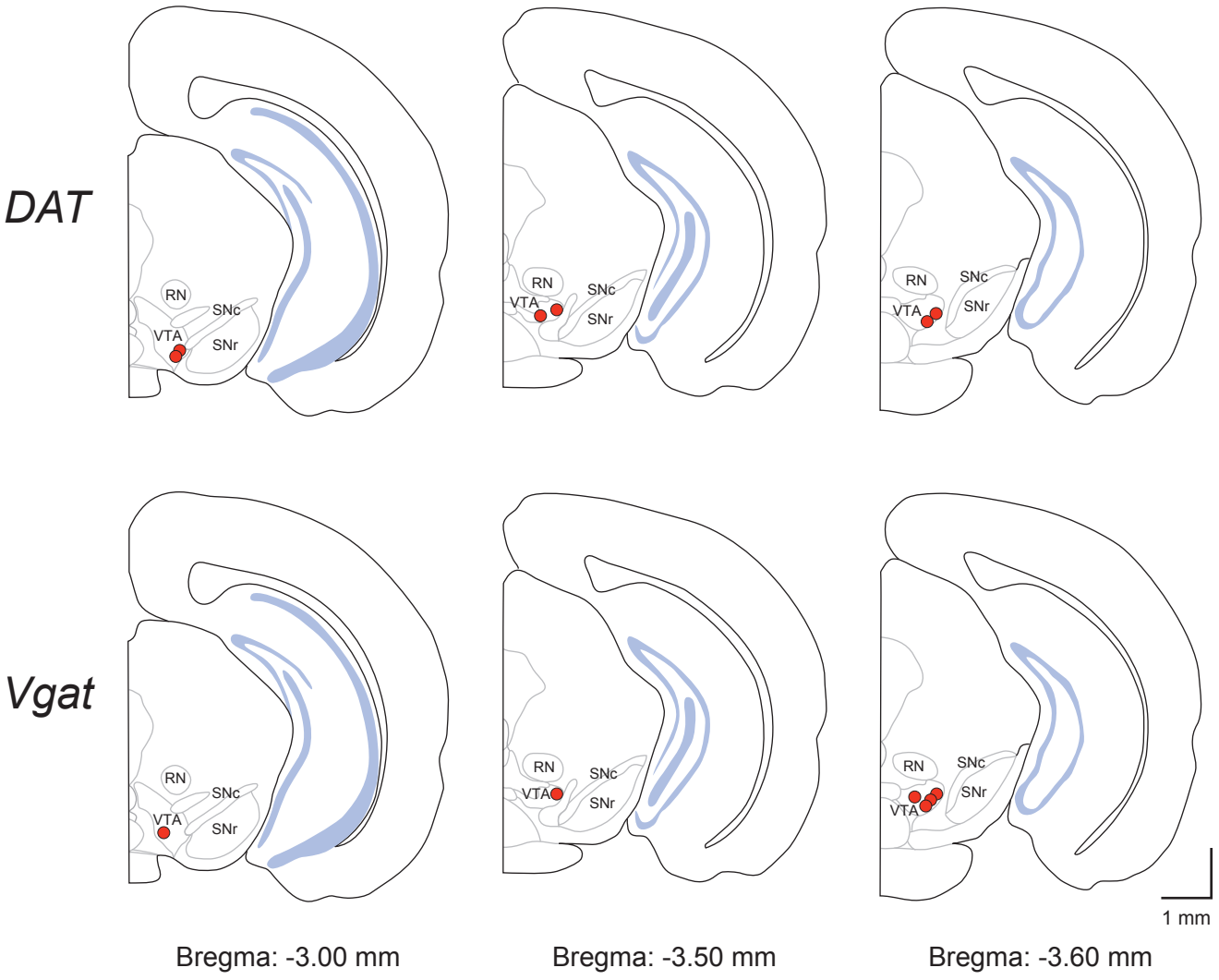

Figure S12. Histological reconstruction of recording sites (red circles). Labeled structures: red nucleus (RN), substantia nigra pars compacta (SNc), substantia nigra pars reticulata (SNr), VTA.

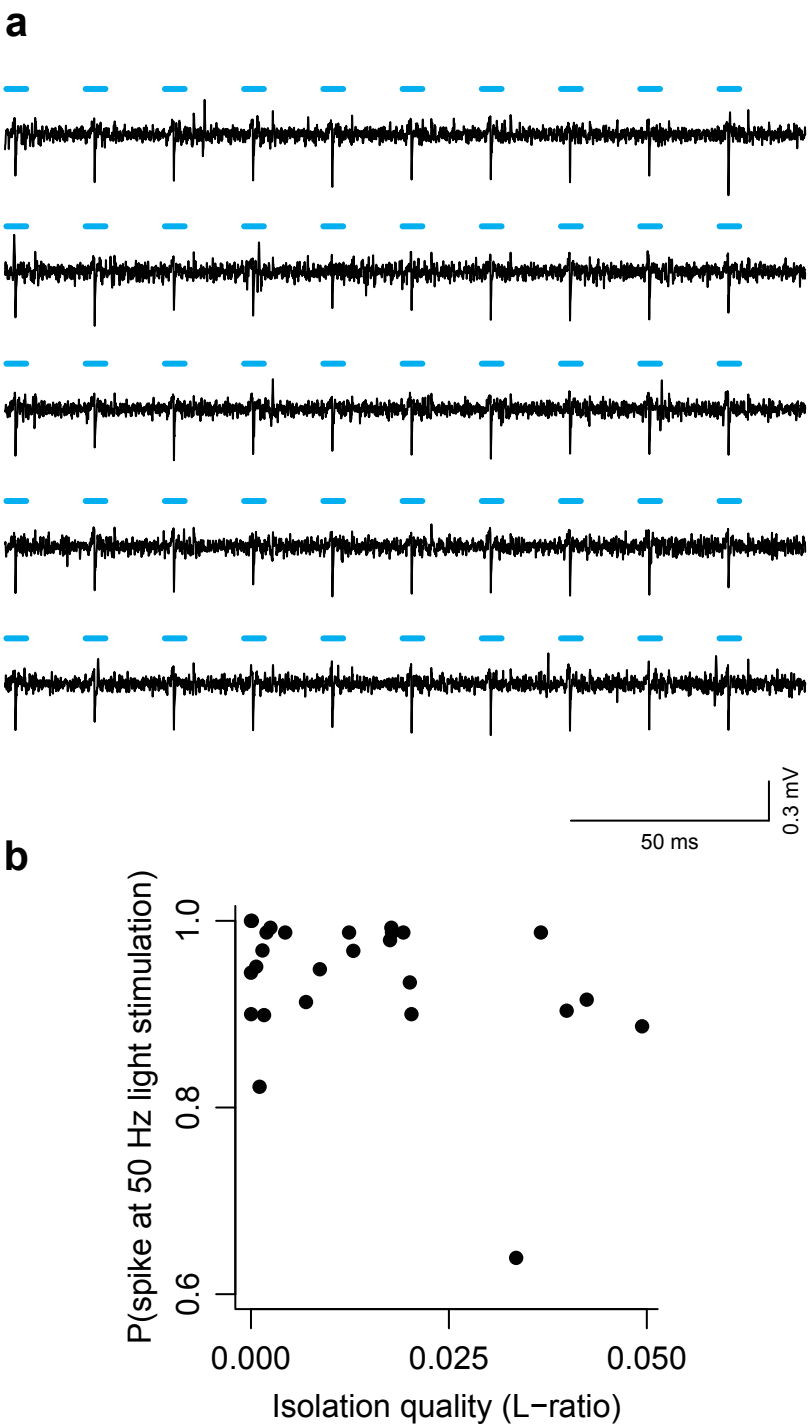

Figure S13. Dopaminergic neurons follow high-frequency light stimulation. **a**, Five consecutive trials of 50 Hz light stimulation from a dopaminergic neuron. **b**, Probability of following 50 Hz stimulation as a function of isolation quality, measured using the L-ratio. Smaller values indicate better isolation. The L-ratio for the example neuron is 3.6×10^{-8}.